

Polar-Coded Non-Coherent Communication

Peihong Yuan, *Student Member, IEEE*, Mustafa Cemil Coşkun, *Student Member, IEEE*,
Gerhard Kramer, *Fellow, IEEE*

Abstract—A polar-coded transmission (PCT) scheme with joint channel estimation and decoding is proposed for channels with unknown channel state information (CSI). The CSI is estimated via successive cancellation (SC) decoding and the constraints imposed by the frozen bits. SC list decoding with an outer code improves performance, including resolving a phase ambiguity when using quadrature phase-shift keying (QPSK) and Gray labeling. Simulations with 5G polar codes and QPSK show gains of up to 2 dB at a frame error rate (FER) of 10^{-4} over pilot-assisted transmission for various non-coherent models. Moreover, PCT performs within a few tenths of a dB to a coherent receiver with perfect CSI. For Rayleigh block-fading channels, PCT outperforms an FER upper bound based on random coding and within one dB of a lower bound.

Index Terms—polar codes, fading channel, blind estimation, non-coherent communication, pilot-assisted transmission

I. INTRODUCTION

THE communication setting where channel state information (CSI) is not available at the transmitter or receiver is known as *non-coherent* communication [1, Ch. 10.7]. A common approach to address the lack of CSI is to embed pilot symbols in the transmitted symbol string, have the receiver estimate the CSI based on the pilots, and use the estimated CSI to decode. This approach is called pilot-assisted transmission (PAT) [2] with mismatched decoding [3, Ex. 5.22], [4]–[8].

PAT has two disadvantages for short block lengths: mismatched decoding reduces reliability and pilot symbols reduce rate significantly at low to moderate signal-to-noise ratio (SNR) [6], [7], [9]–[11]. Both problems can be partially mitigated with sophisticated signal processing. For instance, one may use iterative channel estimation and decoding [12]–[18], or two-stage algorithms that consider pilot symbols as part of the codebook [19], [20], or even maximum likelihood (ML) decoding. Nevertheless, there is a fundamental performance degradation due to using pilot symbols [9].

We propose a pilot-free two-stage polar-coded transmission (PCT) scheme to jointly estimate the CSI and data with an adjustable complexity that can be made comparable to PAT. In the first stage, successive cancellation list (SCL) decoding and the polar code constraints are used to estimate the CSI. In the second stage, mismatched SCL decoding proceeds with this estimate. Gains of up to 2 dB are shown at a frame error rate (FER) of 10^{-4} as compared to classic PAT schemes for several non-coherent settings.

This work was supported by the German Research Foundation (DFG) under Grant KR 3517/9-1, and by the Helmholtz Gemeinschaft through the HGF-Allianz DLR@Uni project Munich Aerospace under the grant “Efficient Coding and Modulation for Satellite Links with Severe Delay Constraints”.

The authors are with the Institute for Communications Engineering of the Technical University of Munich (TUM), Theresienstr. 90, 80333 Munich, Germany (email: {peihong.yuan,mustafa.coskun,gerhard.kramer}@tum.de).

A related method to estimate CSI uses the parity-check constraints of a low-density parity-check (LDPC) code [21], [22]. However, SCL decoding of polar codes naturally provides soft estimates of frozen bits. Moreover, polar codes are usually used with a high-rate outer code [23], [24] that can resolve CSI ambiguities, e.g., the phase ambiguity when using quadrature phase-shift keying (QPSK) and Gray labeling [21]. Of course, one may consider outer codes for LDPC codes as well. Other low-complexity methods for non-coherent channels are described in, e.g., [21], [25]–[28]. We remark that our focus is on QPSK but the ideas extend to higher-order modulations. One may also combine PAT and PCT to optimize performance.

This paper is organized as follows. Sec. II introduces notation, the system model, polar codes, and PAT. Sec. III describes our joint channel estimation and decoding algorithm. Sec. IV demonstrates the effectiveness of the method for short polar codes concatenated with an outer cyclic redundancy check (CRC) code and QPSK. Sec. V concludes the paper.

II. PRELIMINARIES

Uppercase letters, e.g., X , denote random variables and lowercase letters, e.g., x , denote their realizations. The probability distribution of X evaluated at x is written as $P_X(x)$ or $P(x)$ when the argument is the lower-case version of the random variable. We similarly treat densities $p_X(x)$ or $p(x)$. For $a \leq b$ we write x_a^b for the row vector (x_a, \dots, x_b) . Lower case bold letters, e.g., \mathbf{x} , also denote row vectors. Capital bold letters, e.g., \mathbf{X} , denote random vectors. All-zeros and all-ones vectors are denoted as $\mathbf{0}$ and $\mathbf{1}$, respectively. The notation \overline{x}_a^b refers to the element-wise bit-flipped version of a binary vector x_a^b . We write $[N] = \{1, \dots, N\}$ and use calligraphic letters, e.g., \mathcal{S} , for sets otherwise. A subvector $x_{\mathcal{S}}$ of x_1^N is formed by appropriately ordered elements with indices in \mathcal{S} . The cardinality of \mathcal{S} is denoted as $|\mathcal{S}|$. We write $\|\cdot\|$ for the l_2 -norm and $\langle \cdot, \cdot \rangle$ for the inner product of two vectors. Finally, $\mathbb{F}^{\otimes m}$ refers to the m -fold Kronecker product of a matrix \mathbb{F} where $\mathbb{F}^{\otimes 0} = \mathbf{1}$.

A. System Model

Consider a scalar block-fading channel, i.e., the fading coefficient H is constant for n_c channel uses and changes independently across B coherence blocks, resulting in a frame size of $n = Bn_c$ symbols. The channel output of the i th coherence block is

$$\mathbf{y}_i = h_i \mathbf{x}_i + \mathbf{z}_i, \quad i = 1, \dots, B \quad (1)$$

where $\mathbf{x}_i \in \mathcal{X}^{n_c}$ and $\mathbf{y}_i \in \mathbb{C}^{n_c}$ are the transmitted and received vectors, $h_i \in \mathbb{C}$ is a realization of H , and \mathbf{z}_i is an

additive white Gaussian noise (AWGN) term whose entries are independent and identically distributed (i.i.d.) as $\mathcal{CN}(0, 2\sigma^2)$. Neither the transmitter nor the receiver knows h_i or even the probability distribution of H . We assume that the noise variance $2\sigma^2$ is known to the receiver; this may be justified by the slow time scale of receiver device variations as compared to fading due to mobility. A vector without subscripts denotes a concatenation of vectors or scalars, e.g., $\mathbf{y} = (\mathbf{y}_1, \dots, \mathbf{y}_B)$, $\mathbf{x} = (\mathbf{x}_1, \dots, \mathbf{x}_B)$ and $\mathbf{h} = (h_1, \dots, h_B)$.

Consider QPSK with Gray labeling. The input alphabet is $\mathcal{X} = \{\pm\Delta \pm j\Delta\}$, $\Delta > 0$, and we map the binary vector c_1^{2m} to $x_1^m \in \mathcal{X}^m$ via $\chi: \{0, 1\}^{2m} \mapsto \mathcal{X}^m$ as

$$\chi(c_1^{2m}) = (\chi_g(c_1, c_2), \chi_g(c_3, c_4), \dots, \chi_g(c_{2m-1}, c_{2m})) \quad (2)$$

where $\chi_g(c^2) = (-1)^{c_1}\Delta + j(-1)^{c_2}\Delta$. The mapping (2) is symmetric, i.e., if $\chi(c_1^{2m}) = \mathbf{x}$ then $\chi(c_1^{2m}) = -\mathbf{x}$.

B. Polar Codes

A binary polar code of block length N and dimension K is defined by a set $\mathcal{A} \subseteq [N]$ of indices with $|\mathcal{A}| = K$ and the matrix $\mathbb{F}^{\otimes \log_2 N}$, where N is a positive-integer power of 2 and \mathbb{F} is the binary Hadamard matrix [29]. Encoding is performed as $c_1^N = u_1^N \mathbb{F}^{\otimes \log_2 N}$, where the input vector u_1^N has K uniform information bits $u_{\mathcal{A}}$ and $N - K$ frozen bits $u_{\mathcal{F}} = \mathbf{0}$ with $\mathcal{F} = [N] \setminus \mathcal{A}$. A polar code is designed by storing the indices of the most reliable bits under SC decoding in the set \mathcal{A} [29], [30]. In this work, we use the channel quality independent beta-expansion construction [31].

An successive cancellation (SC) decoder estimates the bit u_i at decoding stage i as $\hat{u}_i = 0$ if $i \in \mathcal{F}$, and otherwise

$$\hat{u}_i = \arg \max_{u_i \in \{0, 1\}} p_{\mathbf{Y}, U_1^{i-1} | U_i}(\mathbf{y}, \hat{u}_1^{i-1} | u_i)$$

where the probabilities are approximated recursively by assuming that U_j , $i < j \leq N$, are i.i.d. uniform random bits [29]. Both encoding and SC decoding can be implemented with complexity $\mathcal{O}(N \log_2 N)$ [29].

SCL decoding with list size L runs L instances of an SC decoder in parallel [23]. Each instance has a different hypothesis on the decoded information bits \hat{u}_1^{i-1} at decoding stage i , called a decoding path. After decoding stage N , the decoder outputs the hypothesis of the most likely path as the estimate \hat{u}_1^N . An SCL decoder can be implemented with complexity $\mathcal{O}(LN \log_2 N)$ [23].

Polar codes perform significantly better when combined with an outer CRC code [23]. Decoding proceeds as follows: An SCL decoder for the inner polar code produces a list of codewords. The outer decoder discards those not fulfilling the constraints of the outer code. The decoder puts out the most likely of the remaining codewords if there is at least one, and it declares a frame error otherwise. For classic AWGN channels, these modified polar codes are competitive under SCL decoding for short block lengths [32].

C. Pilot-Assisted Transmission

Consider PAT as shown in Fig. 1 where the first n_p symbols in each coherence block are pilot symbols \mathbf{x}_i^p and

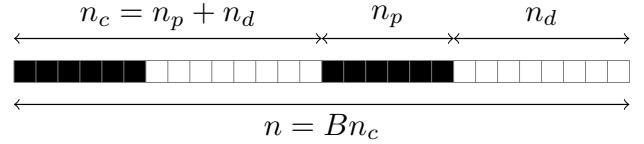


Figure 1. A PAT frame structure with $B = 2$ coherence blocks. Dark and white boxes represent pilot and coded symbols, respectively.

the remaining $n_d = n_c - n_p$ symbols \mathbf{x}_i^d are coded. To keep the overall rate fixed, the (N, K) code is punctured by using quasi-uniform puncturing (QUP) [33] so that the code length after puncturing is $N_{\text{punc}} = N - 2Bn_p = 2Bn_d$ with QPSK. The pilot and coded symbols have the same energy. Upon observing \mathbf{y} , an ML estimate of the CSI is $\hat{h}_i = \langle \mathbf{y}_i^p, \mathbf{x}_i^p \rangle / \|\mathbf{x}_i^p\|^2$. A mismatched decoder uses $\hat{\mathbf{h}} = (\hat{h}_1, \dots, \hat{h}_B)$ to compute the bit-wise log-likelihood ratios (LLRs) that are fed to the SCL decoder, leading to a codeword estimate.

III. JOINT CHANNEL ESTIMATION AND DECODING

This section presents a low-complexity joint channel estimation and decoding scheme for polar codes. We do not use pilot symbols, i.e., we have $n_p = 0$ and $\mathbf{x}_i = \mathbf{x}_i^d$. A random interleaver Π permutes the encoded bits c_1^N and is followed by the mapping (2). The channel model is (1).

Let $h_i = r_i e^{j\theta_i}$ where $r_i \in [0, \infty)$ and $\theta_i \in [0, 2\pi)$, $i \in [B]$. We begin by estimating the amplitudes $r_i = |h_i|$ as

$$\hat{r}_i = \left(\sqrt{2}\Delta \right)^{-1} \sqrt{\frac{1}{n_c} \|\mathbf{y}_i\|^2 - 2\sigma^2}, \quad i = 1, \dots, B. \quad (3)$$

Let β be a number of input bits, and let $\mathcal{A}^{(\beta)} = \mathcal{A} \cap [\beta]$ and $\mathcal{F}^{(\beta)} = \mathcal{F} \cap [\beta]$ be sets of information and frozen indices among the first β input bits u_1^β . We use the polar code constraints to estimate the phase as

$$\begin{aligned} \left\{ \hat{\theta}_1, \dots, \hat{\theta}_B \right\} &= \arg \max_{\{\theta_1, \dots, \theta_B\}} p_{\mathbf{Y} | U_{\mathcal{F}^{(\beta)}}, \mathbf{H}}(\mathbf{y} | \mathbf{0}, \hat{\mathbf{h}}) \\ &= \arg \max_{\{\theta_1, \dots, \theta_B\}} \sum_{u_{\mathcal{A}^{(\beta)}}} p_{\mathbf{Y}, U_{\mathcal{A}^{(\beta)}} | U_{\mathcal{F}^{(\beta)}}, \mathbf{H}}(\mathbf{y}, u_{\mathcal{A}^{(\beta)}} | \mathbf{0}, \hat{\mathbf{h}}) \end{aligned} \quad (4)$$

where $\hat{h}_i = \hat{r}_i e^{j\theta_i}$, $i \in [B]$. The sum in (4) can be computed by SCL decoding up to decoding stage $|\mathcal{F}^{(\beta)}|$ with a list size $L_e = 2^{|\mathcal{A}^{(\beta)}|}$. To reduce complexity at the expense of accuracy, one can approximate the calculation with SCL decoding and L_e satisfying $1 \leq L_e < 2^{|\mathcal{A}^{(\beta)}|}$. In fact, simulations in Sec. IV show that small list sizes such as $L_e = 8$ give FER curves close to those of the coherent receiver.

Remark 1. The search space in (4) grows exponentially in the number of diversity branches B . There are several approaches to reduce complexity and we consider only the symmetry of the likelihood function due to the channel (1) and mapping (2) that halves the search space. We further adopt a coarse-fine search [21], [34] as an efficient optimizer.

Lemma 1. Polar-coded modulations with the mapping (2) and the channel (1) have a sign ambiguity for the channel coefficients, i.e., for all \mathbf{y} , \mathbf{h} and u_1^{N-1} , we have

$$p_{\mathbf{Y} | U_1^N, \mathbf{H}}(\mathbf{y} | (u_1^{N-1}, 0), \mathbf{h}) = p_{\mathbf{Y} | U_1^N, \mathbf{H}}(\mathbf{y} | (u_1^{N-1}, 1), -\mathbf{h}).$$

Proof. For all $\mathbf{x}, \mathbf{y}, \mathbf{h}$ and $\mathbf{s} \in \{-1, +1\}^B$, we have

$$p(\mathbf{y}|\mathbf{x}, \mathbf{h}) = \prod_{i=1}^B p_{\mathbf{Y}_i|\mathbf{X}_i, \mathbf{H}_i}(\mathbf{y}_i|s_i \mathbf{x}_i, s_i \mathbf{h}_i)$$

as $s_i^2 = 1$. Recall that $c_1^N = \Pi^{-1}(\chi^{-1}(\mathbf{x}))$ so that $\overline{c_1^N} = \Pi^{-1}(\chi^{-1}(-\mathbf{x}))$. By choosing $\mathbf{s} = -\mathbf{1}$, we have

$$p_{\mathbf{Y}|\mathbf{C}, \mathbf{H}}(\mathbf{y}|c_1^N, \mathbf{h}) = p_{\mathbf{Y}|\mathbf{C}, \mathbf{H}}(\mathbf{y}|\overline{c_1^N}, -\mathbf{h}). \quad (5)$$

Let u_1^N be the vector such that $c_1^N = u_1^N \mathbb{F}^{\otimes m}$. We have $\overline{c_1^N} = (u_1^{N-1}, \overline{u_N}) \mathbb{F}^{\otimes m}$ because the last row of $\mathbb{F}^{\otimes m}$ is $\mathbf{1}$. \square

Lemma 1 implies that if a polar code is considered for (1), then the decoder cannot resolve the ambiguity on bit u_N . This ambiguity occurs for any binary linear block code that has a generator matrix with an all-ones row, which is reflected in the bit u_N for polar codes.

Theorem 1. Polar-coded modulations with the mapping (2) and the channel (1) satisfy

$$p(\mathbf{y}|u_1^i, \mathbf{h}) = p_{\mathbf{Y}|U_1^i, \mathbf{H}}(\mathbf{y}|u_1^i, -\mathbf{h}) \quad (6)$$

for all \mathbf{y}, \mathbf{h} and $u_1^i, i \in [N-1]$.

Proof. For $i \in [N-1]$, we have

$$\begin{aligned} p(\mathbf{y}|u_1^i, \mathbf{h}) &\stackrel{(a)}{=} \sum_{u_{i+1}^N} P(u_{i+1}^N) p(\mathbf{y}|u_1^N, \mathbf{h}) \\ &\stackrel{(b)}{=} \sum_{u_{i+1}^{N-1}} P(u_{i+1}^{N-1}) \left[\sum_{u_N} \frac{1}{2} p(\mathbf{y}|u_1^N, \mathbf{h}) \right] \\ &\stackrel{(c)}{=} \sum_{u_{i+1}^{N-1}} P(u_{i+1}^{N-1}) \left[\sum_{u_N} \frac{1}{2} p_{\mathbf{Y}|U_1^N, \mathbf{H}}(\mathbf{y}|u_1^N, -\mathbf{h}) \right] \\ &\stackrel{(d)}{=} \sum_{u_{i+1}^N} P(u_{i+1}^N) p_{\mathbf{Y}|U_1^N, \mathbf{H}}(\mathbf{y}|u_1^N, -\mathbf{h}) \end{aligned}$$

where step (a) follows by the law of total probability and the mutual independence of U_1^i, U_{i+1}^N and \mathbf{H} ; steps (b) and (d) follow by rearranging the sums and noting that U_N is uniform; step (c) follows by Lemma 1. \square

Corollary 1. Polar-coded modulations with the mapping (2) and the channel (1) satisfy

$$p_{\mathbf{Y}|U_{\mathcal{F}(\beta)}, \mathbf{H}}(\mathbf{y}|\mathbf{0}, \mathbf{h}) = p_{\mathbf{Y}|U_{\mathcal{F}(\beta)}, \mathbf{H}}(\mathbf{y}|\mathbf{0}, -\mathbf{h}) \quad (7)$$

for all \mathbf{y} and \mathbf{h} .

Proof. We expand

$$\begin{aligned} p_{\mathbf{Y}|U_{\mathcal{F}(\beta)}, \mathbf{H}}(\mathbf{y}|\mathbf{0}, \mathbf{h}) &\stackrel{(a)}{=} \sum_{u_{\mathcal{A}(\beta)}} P(u_{\mathcal{A}(\beta)}) p(\mathbf{y}|u_1^\beta, \mathbf{h}) \\ &\stackrel{(b)}{=} \sum_{u_{\mathcal{A}(\beta)}} P(u_{\mathcal{A}(\beta)}) p_{\mathbf{Y}|U_1^\beta, \mathbf{H}}(\mathbf{y}|u_1^\beta, -\mathbf{h}) \end{aligned}$$

where step (a) follows by the law of total probability and mutually independent $U_{\mathcal{A}(\beta)}, U_{\mathcal{F}(\beta)}$ and \mathbf{H} ; step (b) follows by Theorem 1. \square

Corollary 1 implies that the PCT estimator outputs two solutions for (4), namely $\{\hat{\theta}_1, \dots, \hat{\theta}_B\}$ and $\{\hat{\theta}_1 + \pi, \dots, \hat{\theta}_B + \pi\}$

Algorithm 1: Blind Decoding Algorithm

- 1 **Input:** the received vector \mathbf{y}_1^n .
 - 2 **Output:** the decoded word \hat{u}_A .
 - 1: estimate $\{\hat{r}_1, \dots, \hat{r}_B\}$ via (3)
 - 2: estimate $\{\hat{\theta}_1, \dots, \hat{\theta}_B\} \in [0, 2\pi)^{B-1} \times [0, \pi)$ via (4)
 - 3: run an SCL decoder with the LLRs obtained using $\hat{\mathbf{h}}$ and output the list \mathcal{L} of u_A
 - 4: obtain \mathcal{L}' by flipping the last bit of all $u_A \in \mathcal{L}$
 - 5: among all $u_A \in \mathcal{L} \cup \mathcal{L}'$ that pass the outer code test, choose the most likely one as \hat{u}_A
-

where addition is modulo 2π . An outer code can resolve this ambiguity by optimizing over the set $[0, 2\pi)^{B-1} \times [0, \pi)$ to obtain $\{\hat{\theta}_1, \dots, \hat{\theta}_B\}$ by using the inner code constraints. The demodulator then feeds the SCL decoder with the LLRs. Let \mathcal{L} be the list of words u_A output by the decoder and define

$$\mathcal{L}' = \{(u_{A(N-1)}, \overline{u_N}) : u_A \in \mathcal{L}\}.$$

The outer code now eliminates invalid words in $\mathcal{L} \cup \mathcal{L}'$. Among the survivors, if any, the estimate \hat{u}_1^N is chosen to maximize $p_{\mathbf{Y}|U_1^N, \mathbf{H}}(\mathbf{y}|u_1^N, \hat{\mathbf{h}})$ if $u_A \in \mathcal{L}$ or $p_{\mathbf{Y}|U_1^N, \mathbf{H}}(\mathbf{y}|u_1^N, -\hat{\mathbf{h}})$ if $u_A \in \mathcal{L}'$. An overview is given in Algorithm 1.

Remark 2. An outer code with a minimum distance of at least two can resolve the phase ambiguity.

IV. NUMERICAL RESULTS

This section provides Monte Carlo simulation results to compare the performance of PAT and PCT. The SNR is expressed as E_s/N_0 , where E_s is the energy per symbol and N_0 is the single-sided noise power spectral density. The inner code is a (128, 38) polar code and the outer code is a 6-bit CRC code with generator polynomial $x^6 + x^5 + 1$, resulting in a (128, 32) code. For the QPSK modulator (2) we have $n = Bn_c = 64$ channel uses and an overall rate of $R = 0.5$ bits per channel use (bpcu). For PAT, the (128, 32) code is punctured to obtain Bn_p pilot bits in total, resulting in a $(128 - 2Bn_p, 32)$ code. All curves shown in the figures below are for SCL decoding with a list size of $L = 8$ after estimating the CSI. The optimization (4) uses a coarse-fine search with 8 levels in both the coarse and fine search parts [34]. The performance is compared for various estimator parameters β and L_e and to the coherent receiver with perfect CSI. No puncturing is required for the coherent receiver. As discussed below, the gains of our scheme are similar for $B \in \{1, 2\}$ and with or without fading.

A. Single Coherence Block ($B = 1$)

Consider the channel (1) with $B = 1, r_1 = 1$, and uniformly distributed phase $\Theta_1 \sim \mathcal{U}[0, 2\pi)$. Fig. 2 compares PAT and PCT. The best PAT performance for the FERs of interest was achieved with $n_p = 14$, i.e., 14 pilot symbols gave the lowest SNR for FERs ranging from 10^{-2} to 10^{-4} in Fig. 2. For smaller n_p the quality of the channel estimate limits performance, and for larger n_p the puncturing weakens the polar code and limits performance.

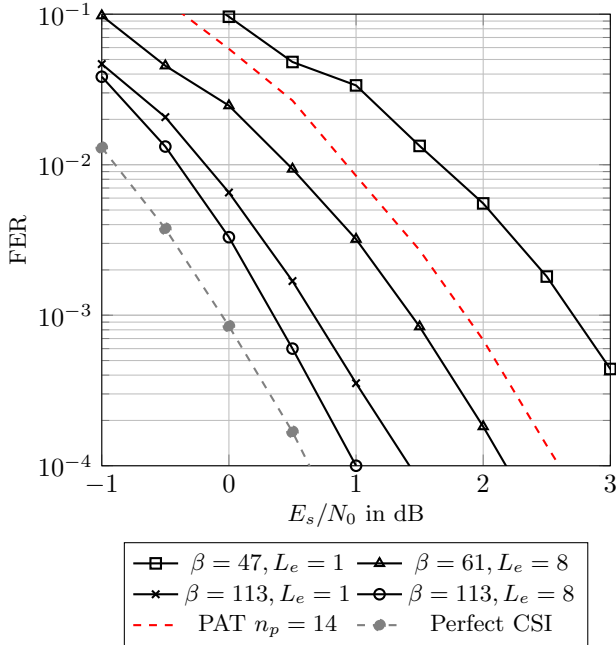


Figure 2. Performance of PAT and PCT for the channel (1) with $B = 1$, $r_1 = 1$, and $\Theta_1 \sim [0, 2\pi)$. A (128, 32) polar code was used with QPSK so that $n = n_c = 64$ and the overall rate is $R = 0.5$ bpcu. SCL decoding uses a list size of $L = 8$ for all cases.

PCT performs within 0.3 dB of the receiver with perfect CSI if the estimator is run with $L_e = 8$ and up to the last frozen bit with $\beta = 113$. It thereby outperforms PAT by about 1.5 dB at a FER of 10^{-4} . Observe that if the estimator is run up to the last frozen bit before the first information bit, i.e., $\beta = 47$, then the performance is worse than for PAT. The parameters $\beta = 113$ and $L_e = 1$ provide a good trade-off between complexity and performance when combined with a second-stage SCL decoding with a list size $L = 8$.

Table I compares the number of visited nodes per frame in the polar decoding tree along with the FER at $E_s/N_0 = 1$ dB. Each visited node corresponds to an input bit (including the frozen bits) visited by the algorithm [35, Remark 4]. For PCT, we state the sum of the number of nodes visited by the estimator and the number of nodes visited by the decoder. The number of visited nodes with PAT and perfect CSI is thus the same. Observe that PCT with $\beta = 113$ and $L_e = 1$ visits a similar number of nodes as PAT with a list size $L = 32$ (the difference is less than 10%) and it reduces the error probability by one order of magnitude. We remark that measuring the complexity by the number of visited nodes is pessimistic for PCT since most of the visited nodes are frozen bits. Hence, simplified SC decoders [36], [37] can significantly reduce complexity.

B. Two Coherence Blocks ($B = 2$)

We next consider $B = 2$ coherence blocks. Fig. 3 shows the FER for $r_i = 1$ and $\Theta_i \sim \mathcal{U}[0, 2\pi)$, $i \in \{1, 2\}$. Fig. 4 shows the FER for a Rayleigh block-fading channel with $H_i \sim \mathcal{CN}(0, 1)$, $i \in \{1, 2\}$. The best performance for PAT was achieved with $n_p = 7$ pilot symbols per coherence block for

Table I
NUMBER OF VISITED NODES PER FRAME AT $E_s/N_0 = 1$ dB

Method	FER	Visited Nodes
PAT ($n_p = 14$, $L = 8$)	8.43×10^{-3}	631
PAT ($n_p = 14$, $L = 32$)	3.16×10^{-3}	2223
PCT ($\beta = 47$, $L_e = 1$, $L = 8$)	3.36×10^{-2}	1383
PCT ($\beta = 61$, $L_e = 8$, $L = 8$)	3.20×10^{-3}	2151
PCT ($\beta = 113$, $L_e = 1$, $L = 8$)	3.50×10^{-4}	2439
PCT ($\beta = 113$, $L_e = 8$, $L = 8$)	1.00×10^{-4}	8807
Perfect CSI ($L = 8$)	2.40×10^{-5}	631

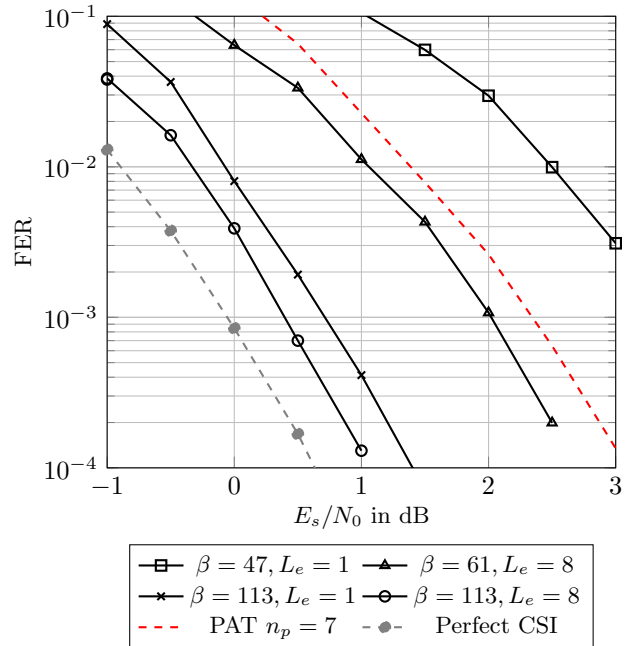


Figure 3. Performance of PAT and PCT for the channel (1) with $B = 2$, $r_i = 1$, and $\Theta_i \sim [0, 2\pi)$ for $i \in \{1, 2\}$. A (128, 32) polar code was used with QPSK so that $n = 2n_c = 64$ and the overall rate is $R = 0.5$ bpcu. SCL decoding uses a list size of $L = 8$ for all cases.

both cases. Observe that, in both cases, PCT outperforms PAT by about 2 dB at a FER $\approx 10^{-4}$. Moreover, PCT approaches the performance of a coherent receiver with perfect CSI.

Fig. 4 also provides an upper (achievability) bound based on the random coding union bound with s parameter (RCUs) [38, Thm. 1] and a lower (converse) bound called a metaconverse (MC) [39, Thm. 28]. Both bounds assume that there is a power constraint per coherence block rather than a codeword. Also, the input distribution is induced by unitary space-time modulation. For more details, see [40].

V. CONCLUSIONS

A PCT scheme was proposed that estimates CSI via SCL decoding and the constraints imposed by the frozen bits. An outer code improves reliability and resolves phase ambiguities. Simulation results show that PCT significantly outperforms PAT schemes with a similar complexity and approaches the performance of a coherent receiver.

ACKNOWLEDGEMENTS

The authors wish to thank Dr. A. Lancho (Chalmers) for providing the RCUs and MC bounds.

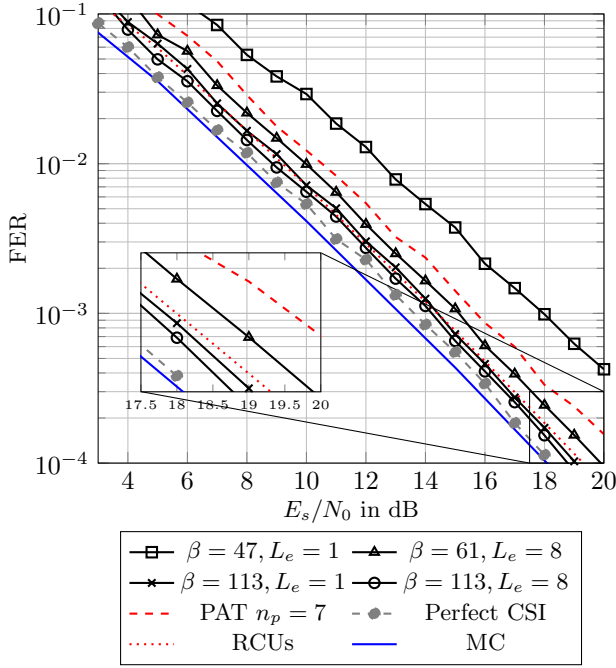


Figure 4. Performance of PAT and PCT for a Rayleigh block-fading channel and $B = 2$. A $(128, 32)$ polar code was used with QPSK and the overall rate is $R = 0.5$ bpcu. SCL decoding uses a list size of $L = 8$ for all cases.

REFERENCES

- [1] E. Biglieri, *Coding for Wireless Channels*. Springer, 2005.
- [2] L. Tong, B. M. Sadler, and M. Dong, "Pilot-assisted wireless transmissions: General model, design criteria, and signal processing," *IEEE Signal Process. Mag.*, vol. 21, no. 6, pp. 12–25, Nov. 2004.
- [3] R. G. Gallager, *Information Theory and Reliable Communication*. John Wiley & Sons, Inc., 1968.
- [4] N. Merhav, G. Kaplan, A. Lapidoth, and S. Shamai Shitz, "On information rates for mismatched decoders," *IEEE Trans. Inf. Theory*, vol. 40, no. 6, pp. 1953–1967, 1994.
- [5] A. Lapidoth and P. Narayan, "Reliable communication under channel uncertainty," *IEEE Trans. Inf. Theory*, vol. 44, no. 6, pp. 2148–2177, 1998.
- [6] G. Taricco and E. Biglieri, "Space-time decoding with imperfect channel estimation," *IEEE Trans. Wireless Commun.*, vol. 4, no. 4, pp. 1874–1888, 2005.
- [7] G. Taricco and G. Coluccia, "Optimum receiver design for correlated Rician fading MIMO channels with pilot-aided detection," *IEEE J. Sel. Areas Commun.*, vol. 25, no. 7, pp. 1311–1321, 2007.
- [8] J. Scarlett, A. Martinez, and A. G. i. Fabregas, "Mismatched decoding: Error exponents, second-order rates and saddlepoint approximations," *IEEE Trans. Inf. Theory*, vol. 60, no. 5, pp. 2647–2666, 2014.
- [9] J. Östman, G. Durisi, E. G. Ström, M. C. Coşkun, and G. Liva, "Short packets over block-memoryless fading channels: Pilot-assisted or noncoherent transmission?" *IEEE Trans. Commun.*, vol. 67, no. 2, pp. 1521–1536, Feb. 2019.
- [10] G. Durisi, T. Koch, and P. Popovski, "Towards massive, ultra-reliable, and low-latency wireless communications with short packets," *Proc. IEEE*, vol. 104, no. 9, pp. 1711–1726, Sep. 2016.
- [11] G. Liva, G. Durisi, M. Chiani, S. S. Ullah, and S. C. Liew, "Short codes with mismatched channel state information: A case study," in *IEEE Int. Workshop on Signal Process. Adv. in Wireless Commun.*, Sapporo, Japan, Jul. 2017, pp. 1–5.
- [12] H. Meyr, M. Moeneclaey, and S. Fechtel, *Digital Communication Receivers: Synchronization, Channel Estimation, and Signal Processing*. Wiley, 1997.
- [13] H. Wymeersch, *Iterative Receiver Design*. Cambridge, 2007.
- [14] C. Herzet, N. Noels, V. Lottici, H. Wymeersch, M. Luise, M. Moeneclaey, and L. Vandendorpe, "Code-aided turbo synchronization," *Proc. IEEE*, vol. 95, no. 6, pp. 1255–1271, 2007.
- [15] N. Noels, C. Herzet, A. Dejonghe, V. Lottici, H. Steendam, M. Moeneclaey, M. Luise, and L. Vandendorpe, "Turbo synchronization: An EM algorithm interpretation," in *IEEE Int. Conf. Commun.*, vol. 4, 2003, pp. 2933–2937 vol.4.
- [16] J. Dauwels and H. A. Loeliger, "Phase estimation by message passing," in *IEEE Int. Conf. Commun.*, vol. 1, 2004, pp. 523–527 Vol.1.
- [17] C. Herzet, V. Ramon, and L. Vandendorpe, "A theoretical framework for iterative synchronization based on the sum-product and the expectation-maximization algorithms," *IEEE Trans. Signal Process.*, vol. 55, no. 5, pp. 1644–1658, 2007.
- [18] M. Khalighi and J. J. Boutros, "Semi-blind channel estimation using the EM algorithm in iterative MIMO APP detectors," *IEEE Trans. Wireless Commun.*, vol. 5, no. 11, pp. 3165–3173, Nov. 2006.
- [19] M. C. Coşkun, G. Liva, J. Östman, and G. Durisi, "Low-complexity joint channel estimation and list decoding of short codes," in *ITG Int. Conf. Syst., Commun. and Coding*, Feb 2019.
- [20] M. Xhemrishi, M. C. Coşkun, G. Liva, J. Östman, and G. Durisi, "List decoding of short codes for communication over unknown fading channels," in *Asilomar Conf. Signals, Systems, Computers*, 2019, pp. 810–814.
- [21] R. Imad, S. Houcke, and M. Ghogho, "Blind estimation of the phase and carrier frequency offsets for LDPC-coded systems," *EURASIP J. Adv. Signal Process.*, vol. 2010, no. 1, pp. 1–13, 2010.
- [22] R. G. Gallager, *Low-density parity-check codes*. Cambridge, MA, USA: M.I.T. Press, 1963.
- [23] I. Tal and A. Vardy, "List decoding of polar codes," *IEEE Trans. Inf. Theory*, vol. 61, no. 5, pp. 2213–2226, May 2015.
- [24] "LS on channel coding," 3GPP TSG RAN WG1 Meeting, R1-1715317, Prague, Czech Republic, Tech. Rep. 90, Aug. 2017.
- [25] D. Warrior and U. Madhow, "Spectrally efficient noncoherent communication," *IEEE Trans. Inf. Theory*, vol. 48, no. 3, pp. 651–668, 2002.
- [26] Rong-Rong Chen, R. Koetter, U. Madhow, and D. Agrawal, "Joint noncoherent demodulation and decoding for the block fading channel: a practical framework for approaching Shannon capacity," *IEEE Trans. Commun.*, vol. 51, no. 10, pp. 1676–1689, 2003.
- [27] G. Coluccia and G. Taricco, "An optimum blind receiver for correlated Rician fading MIMO channels," *IEEE Commun. Lett.*, vol. 11, no. 9, pp. 738–739, 2007.
- [28] B. Matuz, G. Liva, E. Paolini, M. Chiani, and G. Bauch, "Low-rate non-binary LDPC codes for coherent and blockwise non-coherent AWGN channels," *IEEE Trans. Commun.*, vol. 61, no. 10, pp. 4096–4107, 2013.
- [29] E. Arkan, "Channel polarization: A method for constructing capacity-achieving codes for symmetric binary-input memoryless channels," *IEEE Trans. Inf. Theory*, vol. 55, no. 7, pp. 3051–3073, Jul. 2009.
- [30] N. Stolte, "Rekursive Codes mit der Plotkin-Konstruktion und ihre Decodierung," Ph.D. dissertation, TU Darmstadt, 2002.
- [31] G. He, J.-C. Belfiore, I. Land, G. Yang, X. Liu, Y. Chen, R. Li, J. Wang, Y. Ge, R. Zhang *et al.*, "Beta-expansion: A theoretical framework for fast and recursive construction of polar codes," in *IEEE Global Commun. Conf.*, 2017, pp. 1–6.
- [32] M. C. Coşkun, G. Durisi, T. Jerkovits, G. Liva, W. Ryan, B. Stein, and F. Steiner, "Efficient error-correcting codes in the short blocklength regime," *Elsevier Phys. Commun.*, vol. 34, pp. 66–79, Jun. 2019.
- [33] K. Niu, K. Chen, and J.-R. Lin, "Beyond turbo codes: Rate-compatible punctured polar codes," *IEEE Int. Conf. Commun.*, pp. 3423–3427, Jun. 2013.
- [34] D. Rife and R. Boorstyn, "Single tone parameter estimation from discrete-time observations," *IEEE Trans. Inf. Theory*, vol. 20, no. 5, pp. 591–598, 1974.
- [35] M. Jeong and S. Hong, "SC-Fano decoding of polar codes," *IEEE Access*, vol. 7, pp. 81 682–81 690, 2019.
- [36] A. Alamdar-Yazdi and F. R. Kschischang, "A simplified successive-cancellation decoder for polar codes," *IEEE Commun. Lett.*, vol. 15, no. 12, pp. 1378–1380, 2011.
- [37] G. Sarkis, P. Giard, A. Vardy, C. Thibault, and W. J. Gross, "Fast polar decoders: Algorithm and implementation," *IEEE J. Sel. Areas Commun.*, vol. 32, no. 5, pp. 946–957, 2014.
- [38] A. Martinez and A. Guillén i Fabregas, "Saddlepoint approximation of random-coding bounds," in *Inf. Theory Applic. Workshop (ITA)*, San Diego, CA, U.S.A., Feb. 2011.
- [39] Y. Polyanskiy, H. V. Poor, and S. Verdú, "Channel coding rate in the finite blocklength regime," *IEEE Trans. Inf. Theory*, vol. 56, no. 5, pp. 2307–2359, May 2010.
- [40] A. Lancho, J. Östman, G. Durisi, T. Koch, and G. Vazquez-Vilar, "Saddlepoint approximations for short-packet wireless communications," *IEEE Trans. Wireless Commun.*, vol. 19, no. 7, pp. 4831–4846, 2020.